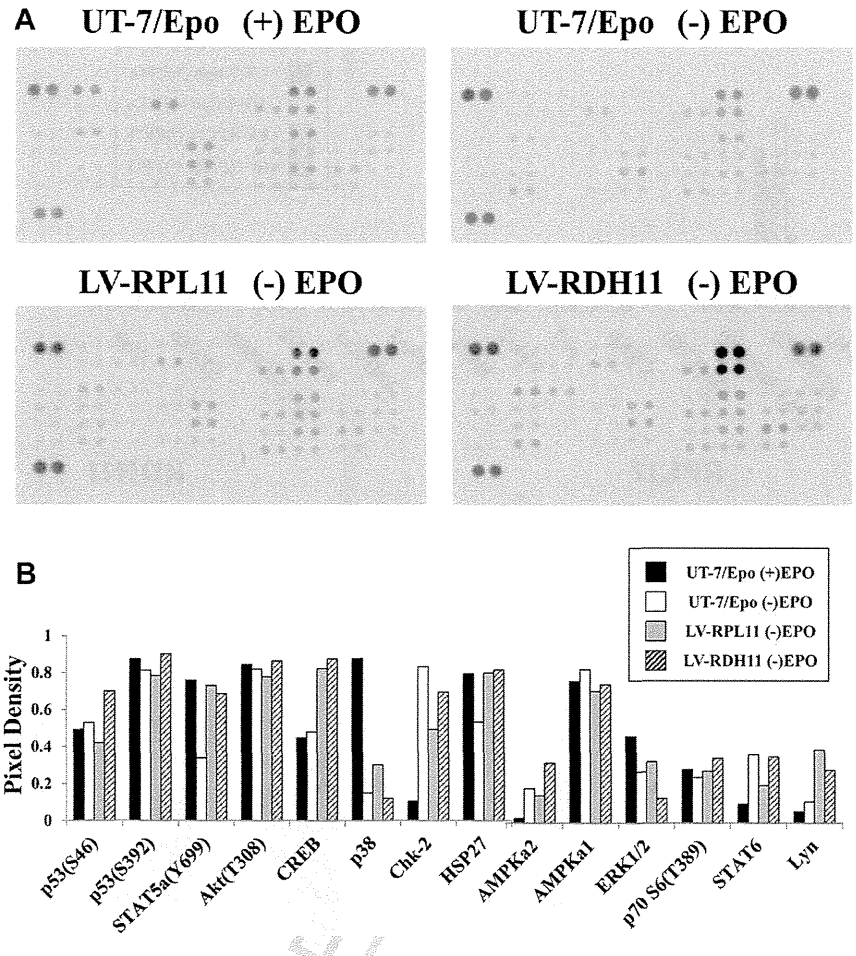

Figure 7. (**A**) Pixel densities of phosphokinase arrays performed on three cell lines. After 12 hours, cells were lysed with lysis buffer and further processed for detection of kinase activation. Pixel densities were evaluated and analyzed using LAS3000 (Fuji Film Co., Tokyo, Japan). (**B**) Determination of signaling pathways in UT-7/Epo and both types of transduced cells. Phosphokinase arrays performed on three cell lines demonstrated that STAT5a (Y699) activation was markedly reduced in UT-7/Epo cultured without Epo, with a pixel density of ~0.4. In UT-7/Epo cultured with Epo, the level of STAT5a (Y699) phosphorylation was almost at the same as in both types of transduced cells cultured with Epo, with a pixel density of ~0.8. The Akt (T308) and AMPKa1 pathways were also activated at almost the same level in all cell lines, with pixel densities of ~0.8. CREB, and Lyn kinases were predominantly activated only in transduced cells, with pixel density ratios (transduced cells vs. UT-7/Epo cells) of ~2.

Discussion

Our findings indicate that the overexpression of RPL11 and RDH11 can maintain the growth and proliferation of UT-7/Epo cells in culture conditions in the absence of Epo. Interestingly, the proliferation of both of RPL11- and RDH11-transduced cells was not due to autocrine manner as shown in Figure 3. Gene transfer of *RPL11* to UT-7/Epo cells resulted in more increased number of cells and colonies than that of *RDH11*. In addition, the percentage of apoptotic cells in RPL11-transduced cells was much lower than that in RDH11-transduced cells. Therefore, it is possible that RPL11 has greater potential than RDH11 to induce the proliferation of UT-7/Epo cells. RPL11 has been recently demonstrated to be essential for normal cell proliferation by supporting ribosomal biogenesis and transcription capacity [9]. In the special context of erythroid proliferation, RPL11 has been previously reported to increase the translation of a specific set of transcripts, such as Bag1, which encodes an Hsp70 cochaperone, and Csde1, which encodes an RNA-binding protein, and both were expressed at increased levels in erythroblasts [10]. A recent report using zebrafish embryos also showed that RPL11 could support hematopoietic iron metabolism and Hb synthesis, whereas the promotion of erythroid proliferation by RDH11 is due to all-*trans*-retinoic acid, an active metabolite of this enzyme's catalytic process [11–13]. As demonstrated in this study, these effects result in promotion of erythroid proliferation by RPL11 and RDH11. Notably, increased expression level of *RDH11* gene in UT-7/Epo cells might not significantly increase the level of retinoic acids produced in these cells, because the substrate for the enzymatic reaction is limited. Moreover, the apoptosis

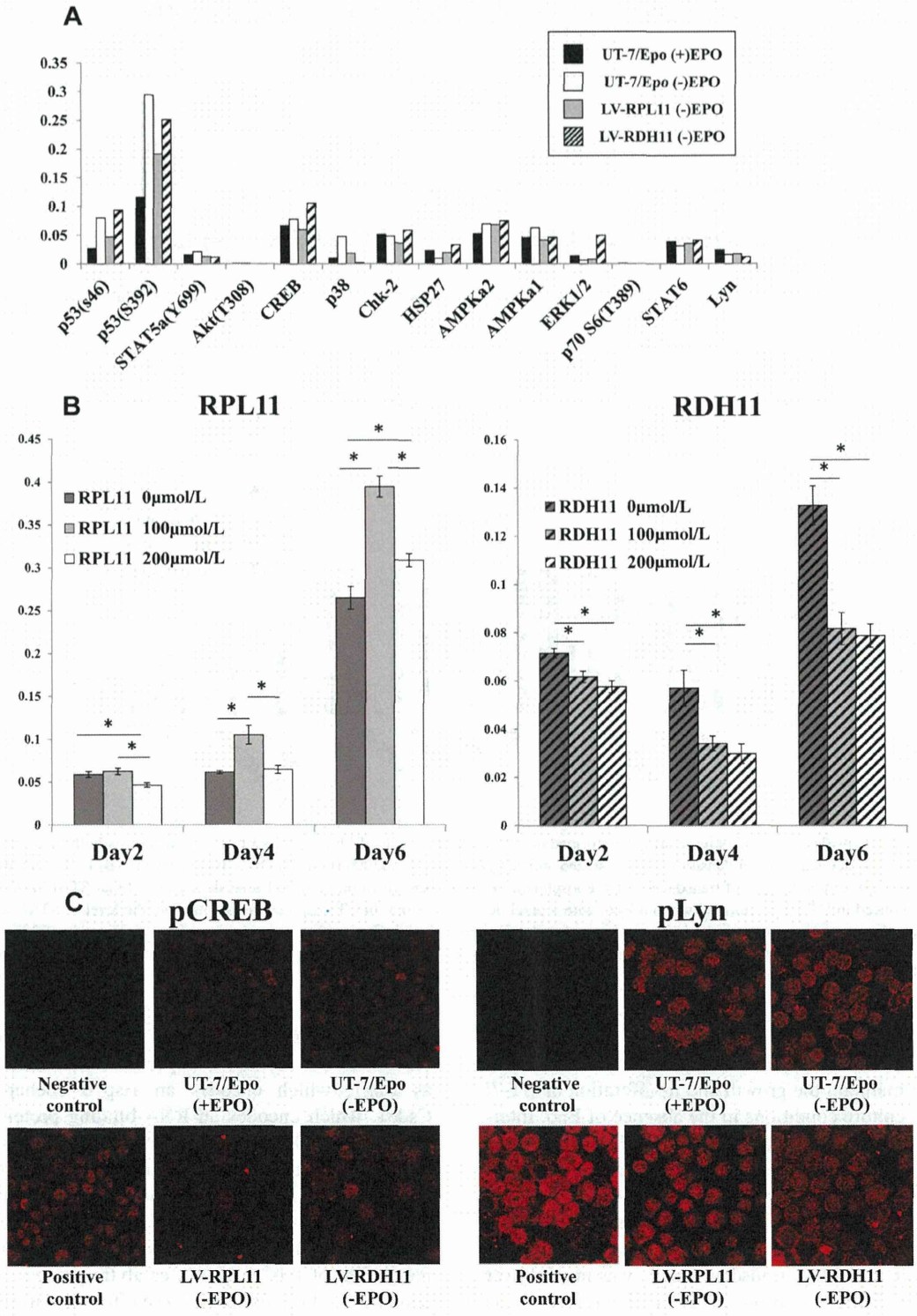

web 4C/FPO

Figure 8. (**A**) Phospho-kinase array with STAT5 inhibitor at a final concentration of 100 μmol/L for 12 hours. To ascertain the STAT5 signaling pathway involved in RPL11- and RDH11-transduced cells, STAT5 inhibitor was added in the culture medium. STAT5a (Y699) was demonstrated to be significantly decreased by phosphokinase array. (**B**) Cell proliferation assays of RPL11- and RDH11-transduced cells with STAT5 inhibitor. RPL11- and RDH11-transduced cells were cultured for 2, 4, and 6 days in the presence of STAT5 inhibitor at final concentrations of 100 and 200 μmol/L. Cells were harvested and processed for proliferation assay. At day 2, the proliferations of RPL11- and RDH11-transduced cells were significantly inhibited at 200 μmol/L of STAT5 inhibitor. * . (**C**) The phosphorylation of CREB and Lyn using immunocytochemistry. UT-7/Epo with or without Epo, and RPL11- and RDH11-transduced cells were harvested and processed for immunocytochemistry. The phosphorylation of CREB and Lyn was demonstrated.

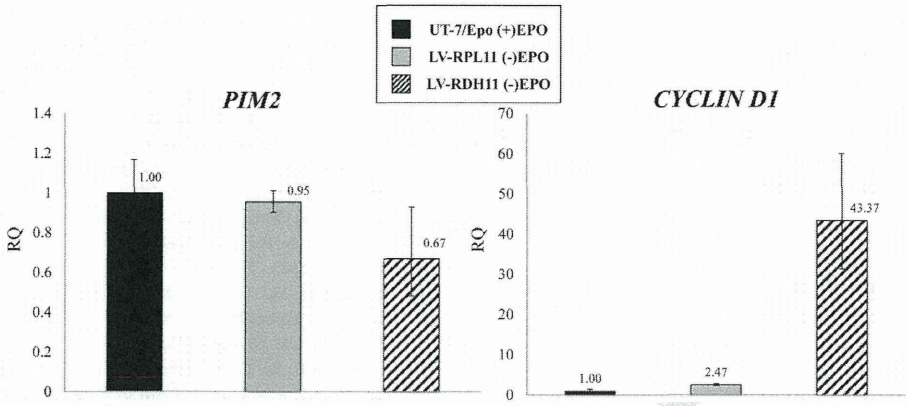

Figure 9. Quantitative RT-PCR of STAT5 target genes. The expression of *PIM2* did not differ significantly among the samples (left). By contrast, *CCND1* was upregulated in RPL11-and RDH11-transduced cells (2.47- and 43.37-fold, respectively) relative to the control UT-7/Epo cells (right). *RQ* = ■■■.

induced by retinoic acid might be another reason that RDH11-transduced cells proliferate less rapidly than those transduced with RPL11 [14]. Only 30% of RPL11- and RDH11-transduced cells could produce â-globin, compared with 80% of UT-7/Epo cells. Several possibilities might explain this reverse switching, including increased expression of specific miRNAs [15–18]. In RDH11-transduced cells, retinoic acid can also inhibit HDACs, resulting in activation of transcriptional processes and ultimately increased expression of γ-globin [19].

Our experiments also demonstrated that STAT5a was markedly activated to almost the same extent in all cell lines, whereas the CREB and Lyn kinases were highly activated in RPL11-and RDH11-transduced cells. Lyn is a hematopoiesis-specific kinase, and its role in erythroid precursors has also been identified. Lyn activation triggers phosphorylation of STAT5 molecules by phosphorylation of protein phosphatase SHP-1 [20,21]. Activation of CREB by the cAMP signaling pathway can also induce STAT5 activation [22,23]. By inhibition of STAT5 activity using STAT5 inhibitor, the proliferation of both RPL11- and RDH11-transduced cells significantly decreased, especially at day 2 with the dosage of 200 μmol/L (Fig. 8B). Thus, it appears that activation of STAT5 was specifically involved in erythroid proliferation in both types of transduced cells, in accordance with a previous report [24]. Surprisingly, our data showed that STAT5 inhibitor could inhibit the proliferation of RPL11-transduced cells, but not as strongly as that of RDH11-transduced cells. This observation indicates that the signaling pathways involving in proliferation of RPL11-transduced cells might be more complex. Moreover, the JAK2 phosphorylation could not be demonstrated in our study. From previous report, JAK2 phosphorylation could be detected for only a 2-hour interval immediately after adding Epo into the Epo-deprived culture medium [25]. Another important possibility is that JAK2 activation is not the upstream signaling pathway of STAT5 in our conditions. Thus, STAT5 phosphorylation in both RPL11- and RDH11-transduced cells may be the direct activation resulting from Lyn and CREB phosphorylation.

The activation of antiapoptotic proteins, BCL-XL and BCL-2, by STAT5 might also be one of the mechanisms that maintains the growth and survival of these cells [26]. Furthermore, *CCND1* expression was highly upregulated in both types of transduced cells, especially in RDH11-transduced cells. STAT5 can induce *CCND1* expression, thereby stimulating cell-cycle progression and further inducing proliferation [27–29]. However, the high accumulation of *CCND1* at day 3 in RDH11-transduced cells might have been due to their active entries from G_0/G_1 to late S phases, concomitant with the accumulation at G_2/M phases, as demonstrated in RDH11 cell cycle determination at 72 hours [27].

In conclusion, our study demonstrates that both of RPL11 and RDH11 can induce proliferation in the UT-7/Epo cell line in the absence of Epo. Our data provide more insights into the mechanisms underlying induction of erythroid proliferation, a promising treatment strategy for patients with conditions such as Diamond–Blackfan anemia (DBA). DBA is caused by mutations of components of the small and large ribosomal subunits, such as RPL5 and RPL11 [30–32]. Therefore, transduction of RPL11 should help to improve patients' symptoms and signs. In addition, transduction of RDH11 results in increased synthesis of all-*trans*-retinoic acid, a potential therapeutic approach for treating the refractory anemia in myelodysplastic syndromes [33]. Our findings also indicate that STAT5 activation is involved in this proliferation process. Finally, CREB and Lyn protein kinases might participate in the activation of STAT5 in our transduced cells, resulting in further upregulation of *CCND1* expression.

Acknowledgement

We are thankful to Ms. Michiko Ushijima for administrative assistance. This work was supported by grants from the Project for Realization of Regenerative Medicine (K.T., 08008010) from the Ministry of Education, Culture, Sports, Science, and Technology (MEXT) of Japan. TK received a grant from the Japan Society for the Promotion of Science (JSPS).

Conflict of interest disclosure

The authors have no competing interests.

References

1. Komatsu N, Yamamoto M, Fujita H, et al. Establishment and characterization of an erythropoietin-dependent subline, UT-7/Epo, derived from human leukemia cell line, UT-7. Blood. 1993;82:456–464.
2. Inoue T, Sugiyama D, Kurita R, et al. APOA-1 is a novel marker of erythroid cell maturation from hematopoietic stem cells in mice and humans. Stem Cell Rev. 2011;7:43–52.
3. Kurita R, Oikawa T, Okada M, et al. Construction of a high-performance human fetal liver-derived lentiviral cDNA library. Mol Cell Biochem. 2008;319:181–187.
4. Stegeman H, Kaanders J, Verheijen M, et al. Combining radiotherapy with MEK1/2, STAT5 or STAT6 inhibition reduces survival of head and neck cancer cells. Mol Cancer. 2013;12:133.
5. Hamadi A, Deramaudt T, Takeda K, Ronde P. Hyperphosphorylated FAK delocalizes from focal adhesions to membrane ruffles. J Oncol. 2010;2010:932803.
6. Uchida M, Kirito K, Endo H, Ozawa K, Komatsu N. Activation of FKHRL1 plays an important role in protecting erythroid cells from erythropoietin deprivation – induced apoptosis in a human erythropoietin-dependent leukemia cell line, UT-7/EPO. Int J Hematol. 2007;86:315–324.
7. Basham B, Sathe M, Grein J, et al. In vivo identification of novel STAT5 target genes. Nucleic Acids Res. 2008;36:3802–3818.
8. Matsumura I, Kitamura T, Wakao H, et al. Transcriptional regulation of the cyclin D1 promoter by STAT5: its involvement in cytokine-dependent growth of hematopoietic cells. EMBO J. 1999;18:1367–1377.
9. Teng T, Mercer CA, Hexley P, et al. Loss of tumor suppressor RPL5/RPL11 does not induce cell cycle arrest but impedes proliferation due to reduced ribosome content and translation capacity. Mol Cell Biol. 2013;33:4660–4671.
10. Horos R, Jspeert H, Pospisilova D, et al. Ribosomal deficiencies in Diamond-Blackfan anemia impair translation of transcripts essential for differentiation of murine and human erythroblasts. Blood. 2012;119:262–272.
11. Zhang Z, Jia H, Zhang Q, et al. Assessment of hematopoietic failure due to Rpl11 deficiency in a zebrafish model of Diamond-Blackfan anemia by deep sequencing. BMC Genomics. 2013;14:896.
12. Liden M, Eriksson U. Understanding retinol metabolism: Structure and function of retinol dehydrogenases. J Biol Chem. 2006;281:13001–13004.
13. Douer D, Koeffler P. Retinoic acid enhances growth of human early erythroid progenitor cells in vitro. J Clin Invest. 1982;69:1039–1041.
14. Noy N. Between death and survival: Retinoic acid in regulation of apoptosis. Annu Rev Nutr. 2010;30:201–217.
15. Lulli V, Romania P, Morsilli O, et al. MicroRNA-486-3p regulates gamma-globin expression in human erythroid cells by directly modulating BCL11A. PLoS One. 2013;8:e60436.
16. Sankaran V, Menne TF, Scepanovic D, et al. MicroRNA-15a and - 16-1 act via MYB to elevate fetal hemoglobin expression in human trisomy 13. Proc Natl Acad Sci U S A. 2011;108:1519–1524.
17. Sankaran V, Orkin S. The switch from fetal to adult hemoglobin. Cold Spring Harb Perspect Med. 2013; http://dx.doi.org/10.1101/cshperspect.a011643.
18. Gabbianelli M, Testa U, Morsilli O, et al. Mechanism of human switching: a possible role of the kit receptor/miR 221-222 complex. Hematologica. 2010;95:1253–1260.
19. Menegola E, Renzo F, Broccia M, Giavini E. Inhibition of histone deacetylase as a new mechanism of teratogenesis. Birth Defects Res C Embryo Today. 2006;78:345–353.
20. Ingley E. Functions of the Lyn tyrosine kinase in health and disease. Cell Commun Signal. 2012;10:21.
21. Xiao W, Ando T, Wang HY, et al. Lyn-and PLC-β3-dependent regulation of SHP-1 phosphorylation controls STAT5 activity and myelomonocytic leukemia-like disease. Blood. 2010;116:6003–6013.
22. Delghandi MP, Johannessen M, Moens U. The cAMP signaling pathway activates CREB through PKA, p38 and MSK1 in NIH3T3 cells. Cell Signal. 2005;17:1343–1351.
23. Boer AK, Drayer AL, Vellenga E. Stem cell factor enhances erythropoietin-mediated transactivation of signal transducer and activator of transcription 5 (STAT5) via the PKA/CREB pathway. Exp Hematol. 2003;31:512–520.
24. Schepers H, Wierenga A, Vellenga E, Schuringa J. STAT5-mediated self-renewal of normal hematopoietic and leukemic stem cells. JAK-STAT. 2012;1:13–22.
25. Erickson-Miller C, Pelus L, Lord K. Signaling induced by erythropoietin and stem cell factor in UT-7/Epo cells: transient versus sustained proliferation. Stem Cell. 2000;18:366–373.
26. Koulnis M, Porpiglia E, Porpiglia P, et al. Contrasting dynamic responses in vivo of the Bcl-XL and Bim erythropoietic survival pathways. Blood. 2012;119:1228–1239.
27. Stacey DW. Cyclin D1 serves as a cell cycle regulatory switch in actively proliferating cells. Curr Opin Cell Biol. 2003;15:158–163.
28. Baldin V, Lukas J, Marcote M, Pagano M, Draetta G. Cyclin D1 is a nuclear protein required for cell cycle progression in G1. Genes Dev. 1993;7:812–821.
29. de Groot RP, Raaijmakers JA, Lammers JW, Koenderman L. STAT5-dependent cyclinD1 and Bcl-XL expression in Bcr-abl transformed cells. Mol Cell Biol Res Commun. 2000;3:299–305.
30. Moniz H, Gastou M, Leblanc T, et al. Primary hematopoietic cells from DBA patients with mutations in RPL11 and RPS19 genes exhibit distinct erythroid phenotype in vitro. Cell Death Dis. 2012;3:e356.
31. Vlachos A, Ball S, Dahl N, et al. Diagnosing and treating Diamond Blackfan anaemia: results of an international clinical consensus conference. Br J Haematol. 2008;142:859–876.
32. Robledo S, Idol R, Crimmins D, Ladenson J, Mason P, Bessler M. The role of human ribosomal proteins in the maturation of rRNA and ribosome production. RNA. 2008;14:1918–1929.
33. Itzykson R, Ayari S, Vassilief D, et al. Is there a role for all-trans retinoic acid in combination with recombinant erythropoietin in myelodysplastic syndromes? A report on 59 cases. Leukemia. 2009;23:673–678.

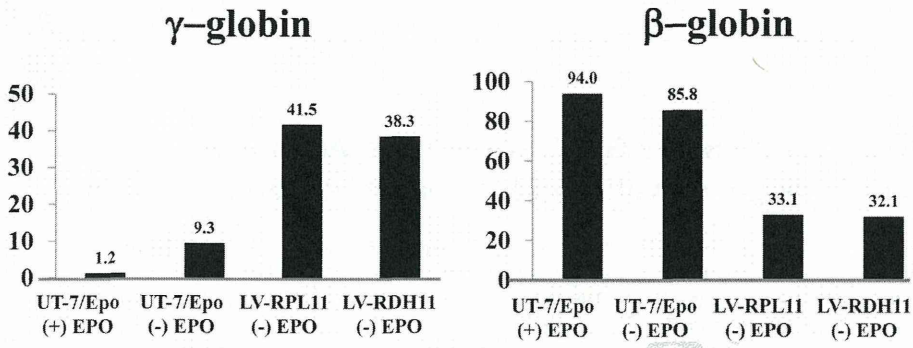

Supplementary Figure 1. Analysis of hemoglobin content in RPL11- and RDH11-transduced cells. Hemoglobin production in both types of transduced cells was compared with that in the parental UT-7/Epo cells. Switching of hemoglobin type was demonstrated to have occurred: adult hemoglobin (β-globin) was highly expressed in UT-7/Epo cells, whereas fetal hemoglobin (γ-globin) was highly expressed in both types of transduced cells.

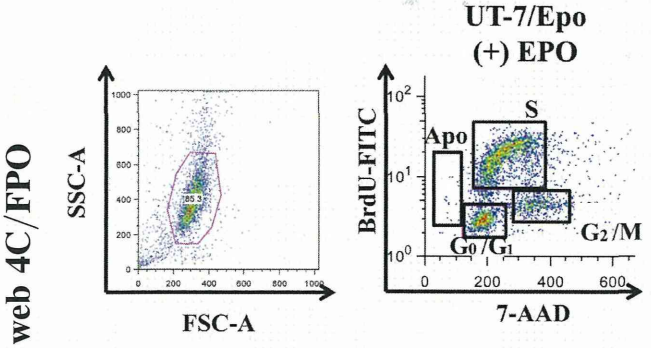

Supplementary Figure 2. Cell cycle determination using FITC-conjugated anti-BrdU, analyzed by flow cytometry of UT-7/Epo cultured with Epo. The G_0/G_1, S, G_2/mol/L, and apoptotic groups were gated as shown.

Published OnlineFirst April 10, 2014; DOI: 10.1158/2326-6066.CIR-13-0143

Research Article

Cancer Immunology Research

TLR7 Ligand Augments GM-CSF–Initiated Antitumor Immunity through Activation of Plasmacytoid Dendritic Cells

Megumi Narusawa[1], Hiroyuki Inoue[1,2,3], Chika Sakamoto[1], Yumiko Matsumura[1], Atsushi Takahashi[1], Tomoko Inoue[1], Ayumi Watanabe[1], Shohei Miyamoto[1], Yoshie Miura[1], Yasuki Hijikata[3], Yoshihiro Tanaka[3], Makoto Inoue[5], Koichi Takayama[2], Toshihiko Okazaki[4], Mamoru Hasegawa[5], Yoichi Nakanishi[2], and Kenzaburo Tani[1,3]

Abstract

Vaccination with irradiated granulocyte macrophage colony-stimulating factor (GM-CSF)–transduced autologous tumor cells (GVAX) has been shown to induce therapeutic antitumor immunity. However, its effectiveness is limited. We therefore attempted to improve the antitumor effect by identifying little-known key pathways in GM-CSF–sensitized dendritic cells (GM-DC) in tumor-draining lymph nodes (TDLN). We initially confirmed that syngeneic mice subcutaneously injected with poorly immunogenic Lewis lung carcinoma (LLC) cells transduced with Sendai virus encoding GM-CSF (LLC/SeV/GM) remarkably rejected the tumor growth. Using cDNA microarrays, we found that expression levels of type I interferon (IFN)–related genes, predominantly expressed in plasmacytoid DCs (pDC), were significantly upregulated in TDLN-derived GM-DCs and focused on pDCs. Indeed, mouse experiments demonstrated that the effective induction of GM-CSF–induced antitumor immunity observed in immunocompetent mice treated with LLC/SeV/GM cells was significantly attenuated when pDC-depleted or IFNα receptor knockout ($IFNAR^{-/-}$) mice were used. Importantly, in both LLC and CT26 colon cancer–bearing mice, the combinational use of imiquimod with autologous GVAX therapy overcame the refractoriness to GVAX monotherapy accompanied by tolerability. Mechanistically, mice treated with the combined vaccination displayed increased expression levels of CD86, CD9, and Siglec-H, which correlate with an antitumor phenotype, in pDCs, but decreased the ratio of $CD4^+CD25^+FoxP3^+$ regulatory T cells in TDLNs. Collectively, these findings indicate that the additional use of imiquimod to activate pDCs with type I IFN production, as a positive regulator of T-cell priming, could enhance the immunologic antitumor effects of GVAX therapy, shedding promising light on the understanding and treatment of GM-CSF–based cancer immunotherapy. *Cancer Immunol Res; 2(6); 568–80. ©2014 AACR.*

Introduction

In recent clinical trials of patients with diverse solid cancers, cancer immunotherapy such as therapeutic vaccination with granulocyte macrophage colony-stimulating factor (GM-CSF) gene-transduced tumor vaccines (GVAX), as well as sipuleucel-T (Provenge; Dendreon), the first FDA-approved GM-CSF–based therapeutic dendritic cell (DC) vaccine for prostate cancer, induced antitumor immune responses with tolerability (1–3). However, the efficacy of this therapy alone is not satisfactory, raising an urgent need to improve the antitumor effect of GVAX. Although GM-CSF signaling is essential in conventional DC (cDC) maturation, which leads to effective generation of tumor-associated antigen (TAA)-specific T cells and differentiation, the underlying molecular mechanism of how GM-CSF sensitizes and matures DCs (GM-DC, i.e., GM-CSF–sensitized DCs) to trigger host antitumor immunity remains unclear.

Therefore, in this study, we attempted to improve the antitumor effects of GVAX therapy through identification of the key cluster genes upregulated in GM-DCs that operate T-cell priming in tumor-draining lymph nodes (TDLN) by conducting a cDNA microarray analysis. We used a syngeneic Lewis lung carcinoma (LLC)–bearing mouse, which exhibited remarkable tumor regression following subcutaneous administration of fusion (F) gene-deleted nontransmissible Sendai virus vector–mediated GM-CSF gene-transduced LLC (LLC/SeV/GM) cells (4). Using this experimental system, the expression microarray analysis elucidated that pathways involving Toll-like receptor 7 (TLR7) and interferon regulatory factor 7 (IRF7), which induce type I interferon (IFN) production in plasmacytoid DCs (pDC; ref. 5), were upregulated in GM-CSF–activated mature DCs. Further activation of this pathway using

Authors' Affiliations: [1]Department of Molecular Genetics, Medical Institute of Bioregulation; [2]Research Institute for Diseases of the Chest, Graduate School of Medical Sciences; [3]Department of Advanced Cell and Molecular Therapy and [4]Center for Clinical and Translational Research, Kyushu University Hospital, Kyushu University, Fukuoka; and [5]DNAVEC Corporation, Tsukuba, Japan

Note: Supplementary data for this article are available at Cancer Immunology Research Online (http://cancerimmunolres.aacrjournals.org/).

Corresponding Author: Kenzaburo Tani, Department of Molecular Genetics, Medical Institute of Bioregulation, Kyushu University, 3-1-1 Maidashi, Higashi-ku, Fukuoka 812-8582, Japan. Phone: 81-92-642-6449; Fax: 81-92-642-6444; E-mail: taniken@bioreg.kyushu-u.ac.jp

doi: 10.1158/2326-6066.CIR-13-0143

Published OnlineFirst April 10, 2014; DOI: 10.1158/2326-6066.CIR-13-0143

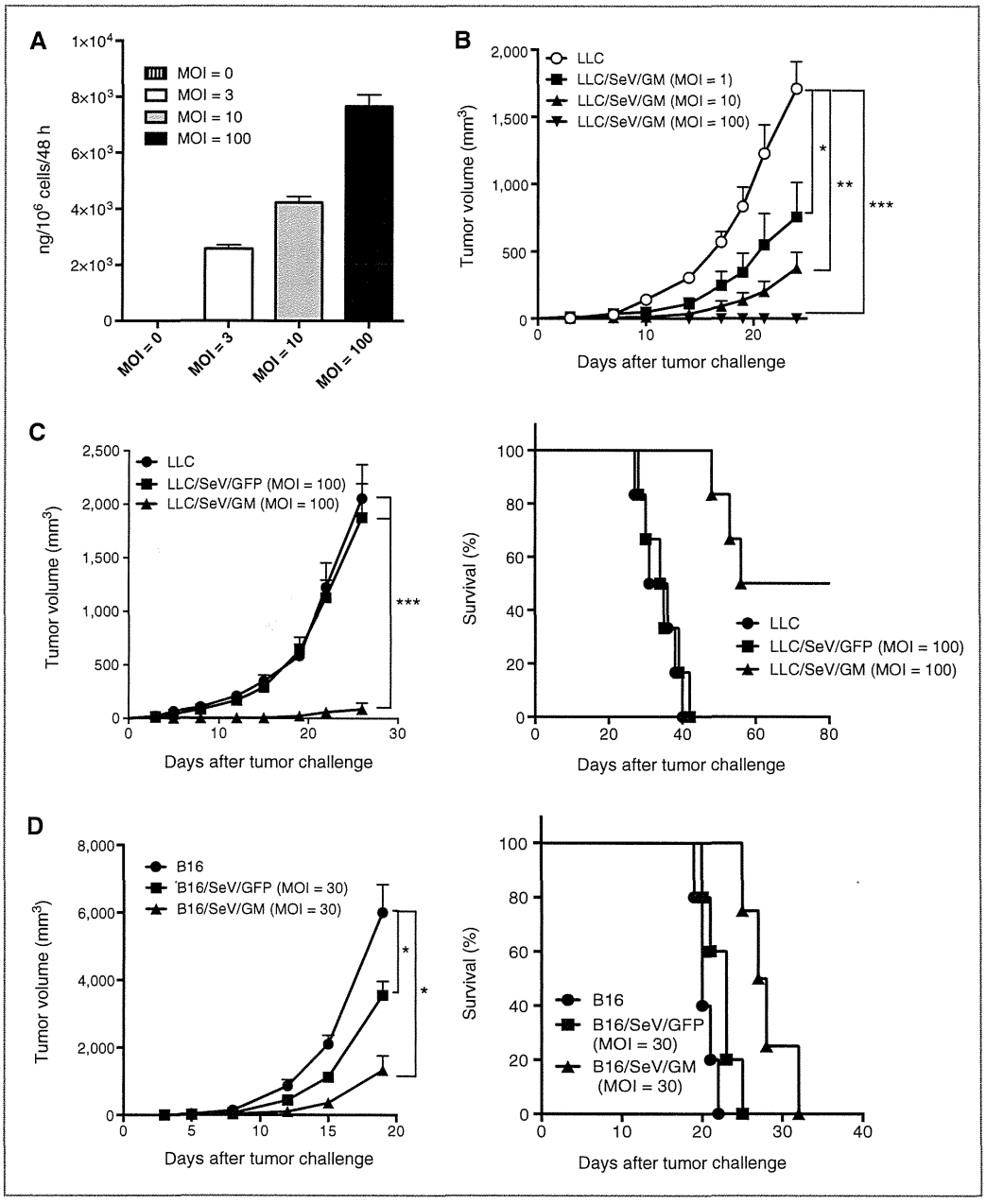

Figure 1. Tumor development of poorly immunogenic LLC and B16F10 cells modified to produce GM-CSF was markedly inhibited. A, dose-escalation studies to assess GM-CSF production from LLC/SeV/GM cells (MOI = 0, 3, 10, and 100). GM-CSF production levels in the supernatants from the 48-hour culture were measured by ELISA. B and C, tumorigenicity assays using LLC cells. B, a total of 3.0×10^5 LLC and LLC/SeV/GM (MOI of 1, 10, or 100) cells were subcutaneously inoculated into the right flank of C57/BL6N mice ($n = 3$). C, a total of 2.0×10^5 LLC, LLC/SeV/GFP, or LLC/SeV/GM (MOI = 100) cells were inoculated into the right flank of C57/BL6N mice ($n = 6$). Significant tumor regression (left) and prolonged survival (right) was shown in mice treated with LLC/SeV/GM cells. D, tumorigenicity assays using B16F10 cells. In total, 1.0×10^5 B16F10, B16/SeV/GFP, or B16/SeV/GM (MOI = 30) cells were inoculated into the right flanks of C57/BL6N mice ($n = 6$). Significant tumor regression (left) and prolonged survival (right) were observed in mice treated with B16/SeV/GM cells. The asterisks indicate statistically significant differences (*, $P < 0.05$; **, $P < 0.01$; ***, $P < 0.001$). Kaplan–Meier survival curves are shown, and mortality was determined by the log-rank test (LLC vs. LLC/SeV/GM and LLC/SeV/GFP vs. LLC/SeV/GM; $P < 0.001$, LLC vs. LLC/SeV/GFP; $P = 0.67$, B16 vs. B16/SeV/GM and B16/SeV/GFP vs. B16/SeV/GM; $P < 0.05$).

Published OnlineFirst April 10, 2014; DOI: 10.1158/2326-6066.CIR-13-0143

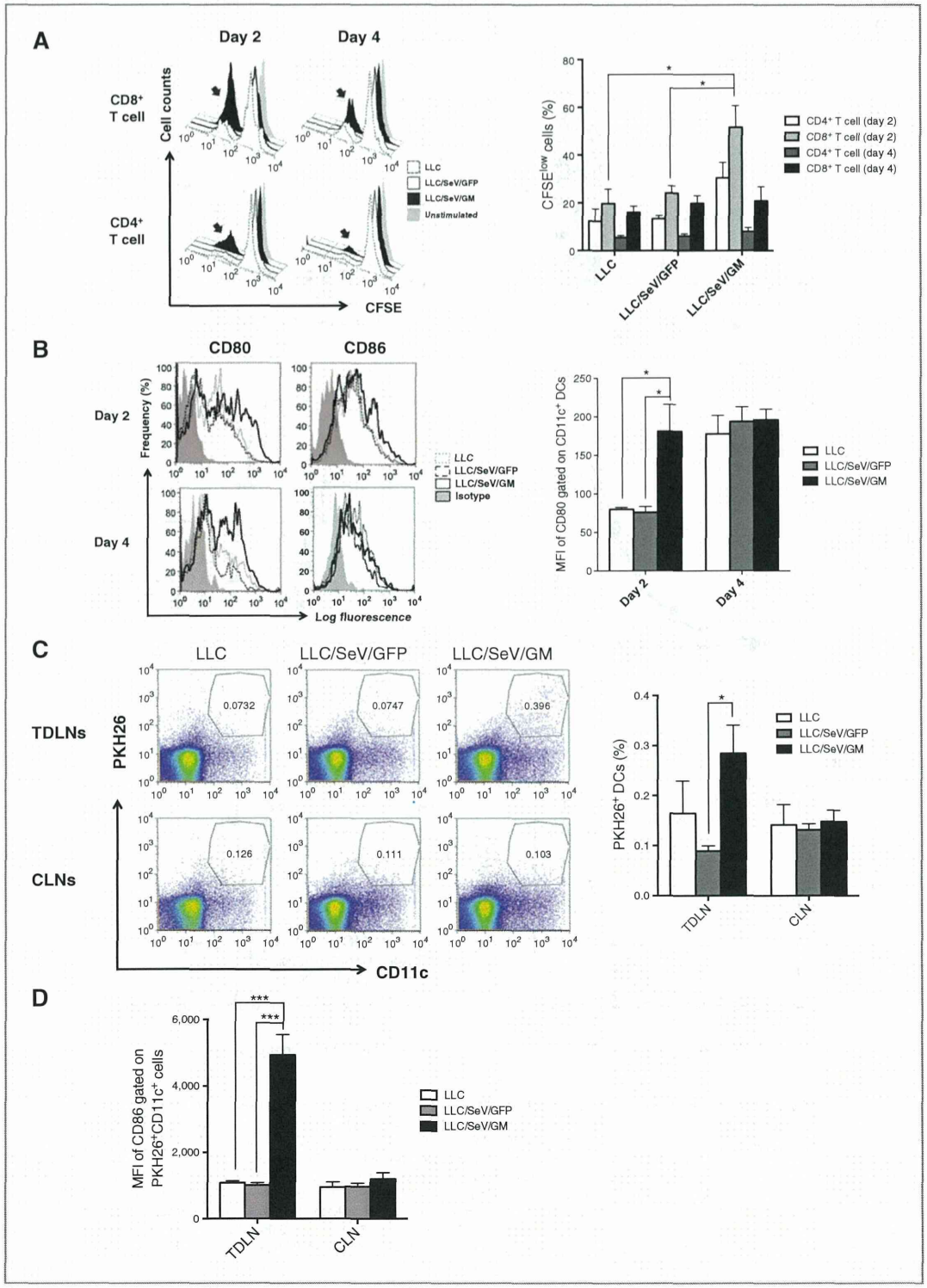

Published OnlineFirst April 10, 2014; DOI: 10.1158/2326-6066.CIR-13-0143

Table 1. Canonical pathways identified by IPA

Pathways	−log (*P* value)	Molecules
Role of pattern recognition receptors in recognition of bacteria and viruses	7.42E+00	OAS1, C3, OAS2, IL6, CCL5, Oas1f, OAS3, IFNA1/IFNA13, TLR2, IFIH1, IRF7, DDX58, TLR7, PIK3R6, EIF2AK2
Pathogenesis of multiple sclerosis	5.33E+00	CXCL10, CXCL9, CCL4, CCL5, CXCL11
Activation of IRF by cytosolic pattern recognition receptors	4.38E+00	DHX58, IFIH1, IRF7, DDX58, ZBP1, STAT2, IL6, IFIT2, IFNA1/IFNA13, ISG15
IFN signaling	3.96E+00	IFIT3, IFIT1, OAS1, MX1, IFI35, STAT2, IFNA1/IFNA13
DC maturation	3.01E+00	FCGR2A, HLA-DMB, IL6, MAPK13, FCGR2B, TREM2, IFNA1/IFNA13, FCGR1A, TLR2, COL1A2, IL1RN, FSCN1, PIK3R6, STAT2
Hepatic fibrosis/hepatic stellate cell activation	2.58E+00	COL1A2, CXCL3, FN1, CXCL9, IGF1, PDGFA, CCL21, CD14, MMP13, CCL5, IL6, IFNA1/IFNA13
Role of hypercytokinemia/hyperchemokinemia in the pathogenesis of influenza	2.49E+00	CXCL10, CCL4, IL1RN, CCL5, IL6, IFNA1/IFNA13
Communication between innate and adaptive immune cells	2.47E+00	CXCL10, TLR2, CCL4, IL1RN, TLR7, CCL5, IL6, IFNA1/IFNA13, Ccl9
Role of tissue factor in cancer	2.45E+00	F10, PDIA2, PIK3R6, HCK, MMP13, F7, LIMK2, MAPK13, FGR, F2
LXR/RXR activation	2.26E+00	APOE, SCD, C3, MSR1 (includes EG:20288), IL1RN, LPL, CLU, CD14, IL6, GC

TLR7 agonist enhanced the therapeutic antitumor effects of GVAX therapy using irradiated autologous GM-CSF gene-transduced vaccine cells in both LLC and CT26 tumor-bearing mouse models with augmented pDC activation. These results showed that the combination of GVAX and imiquimod is an effective therapeutic strategy for cancer immunotherapy, and indicate that activated pDCs have a critical role in the GM-CSF–induced induction of antitumor immunity.

Materials and Methods

Mice

Five- to 10-week-old female immunocompetent C57/BL6N and BALB/cN mice were purchased from Charles River Laboratories Japan and housed in the animal maintenance facility at Kyushu University (Fukuoka, Japan). Type I IFN receptor knockout ($IFNAR^{-/-}$) mice were purchased from The Jackson Laboratory. All animal experiments were approved by the Committee of the Ethics on Animal Experiments in the Faculty of Medicine, Kyushu University. Mouse experiments were carried out at least twice to confirm results.

Tumor cell lines

LLC and CT26 cells were purchased from the American Type Culture Collection (ATCC) and passaged for 3 to 4 months after resuscitation. The mouse melanoma cell line (B16F10) was a kind gift from Dr. Shinji Okano (Kyushu University) and was validated as free from *Mycoplasma* infection; no other validations were performed. Both LLC and CT26 cells were validated as free from *Mycoplasma* infection. No other validations were performed; besides, the former were found as free from ectromelia virus. LLC and B16F10 cells were maintained in Dulbecco's Modified Eagle Medium (DMEM; Nakalai Tesque) supplemented with 10% heat-inactivated fetal bovine serum (FBS) and 1% antibiotic mixture (Nakalai Tesque). CT26 was maintained in RPMI-1640 (Nakalai Tesque) supplemented with 10% FBS and 1% antibiotic mixture.

Gene transduction with nontransmissible recombinant Sendai virus vectors

LLC, B16F10, or CT26 cells were infected with nontransmissible Sendai virus vectors encoding green fluorescence protein (GFP) or mouse GM-CSF (SeV/GFP or SeV/GM, respectively), which were prepared by DNAVEC Corp. (6), at the indicated multiplicity of infection (MOI) for 90 minutes (termed as LLC/SeV/GFP, LLC/SeV/GM, B16/SeV/GFP, B16/SeV/GM, or CT26/SeV/GM cells, respectively). They were cultured for 48 hours after viral gene transduction and used for following mouse studies.

Figure 2. GM-CSF–sensitized DCs elicited superior capacities to stimulate T-cell proliferation and to mobilize TAA-phagocytosed mature DCs into TDLNs. A, CFSE-labeled allogeneic MLR assay. Irradiated $CD11c^+$DCs from mice treated with indicated tumor challenge were mixed with CFSE-labeled allogeneic T cells. After 3 days of coculture, the proliferation rates of T cells were assessed by flow cytometric analysis. Representative histograms depict CFSE expression of allogeneic $CD4^+CD3^+$ or $CD8^+CD3^+$ T cells (left). Bar graphs, mean + SEM percentage of CFSE-diluted cells/total indicated T cells (right). B, representative histograms depict frequency distributions of MFI of CD80 or CD86 expression in $CD11c^+$ DCs from indicated mouse groups on day 2 or 4 after the tumor challenge (left). Bar graphs, mean + SEM of MFI of CD80 on DCs in TDLNs (right). C, representative dot plots show $PKH26^+CD11c^+$ cells gated by their FSC/SSC profiles in TDLNs or CLNs (left). Bar graphs, mean + SEM of percentage of $CD11c^+PKH26^+$ cells in TDLNs or CLNs (right). D, bar graphs, mean + SEM of MFI of CD86 expression levels in $PKH26^+CD11c^+$ cells (*, $P < 0.05$; ***, $P < 0.001$).

Published OnlineFirst April 10, 2014; DOI: 10.1158/2326-6066.CIR-13-0143